LETTER

Friction of a sphere rolling down a granular slope

A Letters Journal Exploring the Frontiers of Physics

September 2018

EPL, **123** (2018) 54005 www.epljournal.org
doi: 10.1209/0295-5075/123/54005

Friction of a sphere rolling down a granular slope

B. Darbois Texier[1], A. Ibarra[1], F. Vivanco[1], J. Bico[2] and F. Melo[1]

[1] *Departamento de Física de la Universidad de Santiago de Chile - Avenida Ecuador 3493, 9170124 Estación Central, Santiago, Chile*
[2] *Sorbonne Université, Université Paris Diderot and Laboratoire de Physique et de Mécanique des Milieux Hétérogenes (PMMH), CNRS, ESPCI Paris, PSL Research University - 10 rue Vauquelin, 75005 Paris, France*

received 7 May 2018; accepted in final form 7 September 2018
published online 8 October 2018

PACS 45.70.-n – Classical mechanics of discrete systems: Granular systems
PACS 81.05.Rm – Porous materials; granular materials
PACS 07.79.Sp – Friction force microscopes

Abstract – The present study investigates the rolling motion of a rigid sphere moving down a granular slope. We observe that the sphere only moves steadily beyond a critical inclination that depends on the diameter and density of the sphere. The groove created on the bed surface during the passage of the sphere, grows with the diameter and density of the sphere and it is nearly independent of both the sphere speed and the slope angle. The granular resistance experienced by the rolling sphere is deduced from its dynamics. A mechanical description of the interaction between the sphere and the granular bed accounts for the experimental findings through a single adjustable parameter. A phase diagram for the sphere dynamics defined by two dimensionless parameters, namely the slope angle and the ratio of the densities of the sphere and of the grains, is proposed.

Introduction. – The scientific questions associated with rolling friction on granular beds are crucial for understanding motorized locomotion on sandy environments, the evolution of talus [1], ballistics of spherical asteroid landers [2] and even the rolling of heavy dung balls in soft soils by beetles [3]. This phenomenon has benefited from a revival of interest after the incident of the rover *Curiosity*, developed by the NASA for Martian exploration, that got stuck for two weeks in a sand dune in 2005. Moreover, the need of robust technological solutions aimed at exploring deformable grounds has motivated the development of instrumented spheres that are propelled by winds similarly as tumbleweeds [4,5]. This solution has been also adapted to polar explorations [6] and reforestation of arid zones. However, the success of these instrumented spheres in the exploration of complex environments requires a deep knowledge of the interaction between the non-cohesive substrates and the sphere. Historically, the problem of rolling friction on a deformable bed has been addressed by Bekker from the point of view of soils mechanics [7,8]. Bekker expressed the drag of a wheel on a flat granular substrate as a function of its geometry, load and empirical soil constants deduced from soil tests. Although this approach has proven effective in practical situations, physical understanding is still missing. More recently, Van wal *et al.* studied experimentally and numerically the rolling resistance of a light sphere on a horizontal granular bed [2]. They developed a theoretical model based on the micro-collisions between the sphere and the ground to account for the rolling friction that partially agrees with their experimental observations. Beyond flat substrates, the case of sandy slopes has been studied by Crassous *et al.* in the context of ants captured inside antlions sand traps [9]. They show that the friction of a slider on a granular bed exhibits large deviations from the Amontons-Coulomb laws at small applied pressure. Predicting the frictional behaviors on inclined granular slopes thus requires new physical laws that remain to be found. The problem of the rolling resistance of dense spheres on an inclined sand bed has been addressed by De Blasio and Saeter [10]. It was observed that the penetrating depth and the rolling friction of the spheres both increase with their density. Since this study was limited to a single slope angle, more experimental efforts are required to achieve a complete physical description of the problem. Here, we investigate systematically the dynamics of spheres rolling

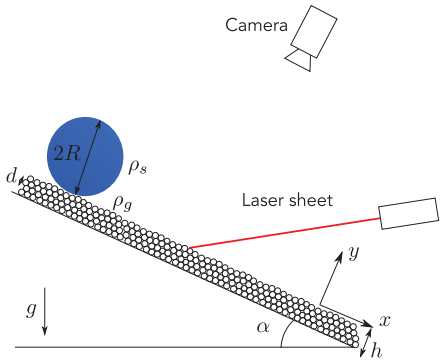

Fig. 1: (Color online) Sketch of the experimental setup.

down an inclined surface of a non-cohesive granular sample. The first section describes the experimental setup and the inferred sphere dynamics. The drag of the sphere is estimated as a function of the slope angle and the main physical parameters. Simultaneously, the deformation of the granular bed due to the passage of the sphere is characterized through the deflection of a laser sheet. In the second part, a simple mechanical model for the rolling resistance on a granular bed is proposed and compared to our experiments. This model accounts for a gradual increase of the asymmetry of the stress distribution acting on the area of the sphere in contact with the bead as the slope is increased. Finally, the different behaviors of the sphere on a granular bed are discussed and summarized in a phase diagram constructed with the slope angle and the ratio of the densities of the sphere and of the grains.

Experiments. – The experiment consists in releasing a homogeneous sphere of radius R and density ρ_s over a flat granular bed made of glass particles of diameter $d = 0.5\,\mathrm{mm}$ (polydispersity of 15%) and tilted by an angle α from the horizontal direction (fig. 1). Spheres are made of expanded polystyrene foam and have a smooth surface in comparison to the grain size. The granular bed is prepared by pouring grains on a horizontal substrate covered with sandpaper and increasing its slope up to an angle $\alpha_a = 23°$ at which an avalanche starts. Once the avalanche stops, a granular layer of constant thickness $h \simeq 10\,\mathrm{mm}$ remains and covers the substrate. According to the study of Pouliquen and Forterre [11], the height of the granular layer, h depends solely on the slope angle, which allows for the preparation of layers of well-defined thickness and good homogeneity. We verified that increasing the thickness of the granular layer does not affect the dynamics of the sphere, indicating that our experiments correspond to the limit of deep granular beds ($h > 4\,\mathrm{mm}$). The bulk density of this preparation has been measured to be $\rho_g = 1540\,\mathrm{kg/m^3}$, corresponding to a packing fraction of $\phi = 0.58$. Thereafter, the slope of the system is reduced to the desired angle α at which the experiment is conducted. The sphere is released at null height above the granular bed without initial velocity or spin. Within

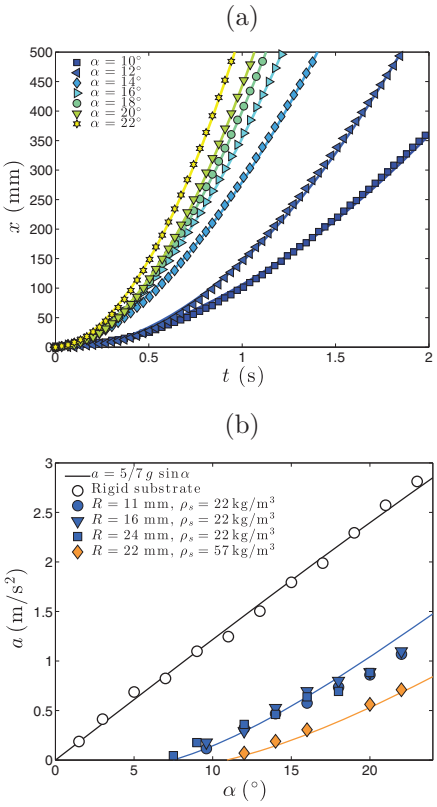

Fig. 2: (Color online) (a) Position of a sphere as a function of time for different slope angles α. The sphere diameter is $R = 16\,\mathrm{mm}$ and its density $\rho_s = 22\,\mathrm{kg/m^3}$. Grains are made of glass beads of mean diameter $d = 0.5\,\mathrm{mm}$ (the polydispersity is about 15%) and the bulk density of the bed is $\rho_g = 1540\,\mathrm{kg/m^3}$. The granular layer is prepared by bringing the system to $\alpha = 23°$ and waiting for the layer to reach the equilibrium thickness of $h \simeq 10\,\mathrm{mm}$. Solid lines correspond to quadratic fits of the form $x = at^2/2$. (b) Acceleration of the sphere as a function of the slope angle α for different sphere diameters ($R = 11$, 16, 24, 22 mm for colored dots, triangles, squares and diamonds, respectively) and densities ($\rho_s = 22$, $57\,\mathrm{kg/m^3}$ for blue and yellow symbols). The dark solid line represents the classical theory for rolling without sliding for a homogeneous sphere ($a = 5/7g\sin\alpha$). The open dots correspond to the case of a sphere rolling on a rigid incline.

the range of sphere radius and density, selected for the experiments, the sphere does not sink entirely into the granular layer and rolls down the incline. The dynamics of the sphere along the slope is captured at a rate of 30 fps through a CCD camera located one meter above the granular layer, preventing optical distortions. The sphere motion is extracted from movies analysis through a MATLAB code based on image correlation.

The typical dynamics of a sphere rolling on the granular slope (fig. 2) reveals that the falling acceleration increases with α and that data are well described by a quadratic law $x = at^2/2$ (solid lines in fig. 2(a)), where a is the acceleration of the sphere that is approximately constant during a fall. Similar experiments were reproduced with

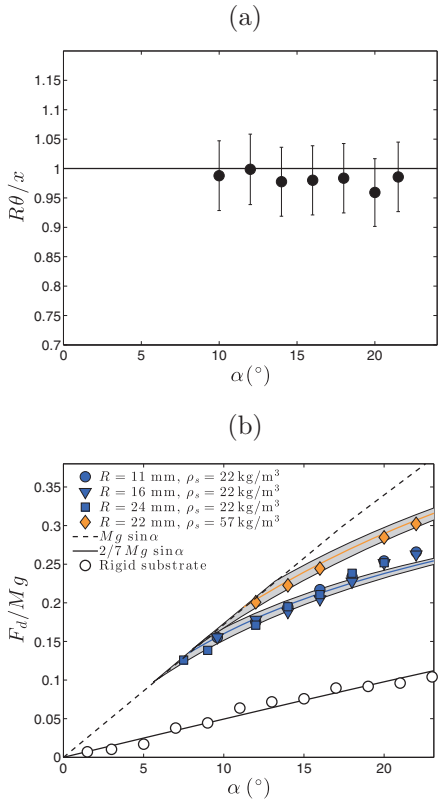

Fig. 3: (Color online) (a) Rolling ratio $R\theta/x$ as a function of the slope α for a sphere of diameter $R = 24\,\mathrm{mm}$ and density $\rho_s = 22\,\mathrm{kg/m^3}$ over a granular bed made of glass beads. The black solid line indicates the classical case of pure rolling. (b) Granular reduced friction F_d/Mg deduced from experimental accelerations and eq. (1). Symbols have the same signification as in fig. 2(b). The blue and yellow solid lines show the prediction of eq. (8) for $c = 1.5$. Gray regions show the model predictions for $c = 1.5 \pm 0.2$. The dark solid line represents the tangential force in the classical case of a pure-rolling motion on a rigid substrate ($F_d = 2/7Mg\sin\alpha$).

spheres of different diameters and densities. In all cases, good fit of experimental data was achieved and the mean acceleration of the sphere, a, was deduced.

Figure 2(b) indicates that a minimal slope angle α_c is required for the sphere to initiate spontaneously its motion. For $\alpha > \alpha_c$, the acceleration of the sphere increases with α and shows vanishing dependency on R (blue symbols in fig. 2(b)). Increasing the sphere density ρ_s results in increasing α_c and reducing the sphere acceleration a. For a given angle, the measured acceleration is significantly lower than the one expected for the classical problem of a sphere rolling without sliding ($a = 5/7g\sin\alpha$, cf. dark solid line and open dots in fig. 2(b)). Thereafter, we investigate the rotation of the sphere while rolling down the granular slope by means of black painted stripes on the sphere surface. Tracking these stripes provides the sphere rotation angle θ recovered while it travels over a given distance x. We observe that the ratio $R\theta/x$ is equal to unity within the experimental accuracy of this study (fig. 3(a)).

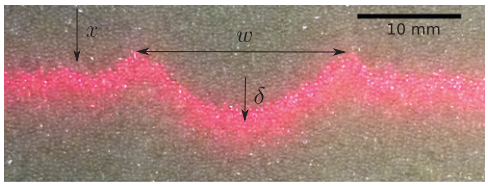

Fig. 4: (Color online) Top view of the deflection of a laser beam at the boundary of the groove produced by the passage of a rolling sphere on a granular bed. The x-direction goes from top to bottom.

We thus conclude that the sphere does not significantly slide. The difference in sphere acceleration compared to the case of a flat and rigid substrate is then attributed to the friction of the sphere due to the deformation of the granular bed. Introducing the friction force F_d experienced by the sphere along the x-direction, the equation of motion yields

$$\frac{\ddot{x}}{g} = \sin\alpha - \frac{F_d}{Mg}, \tag{1}$$

where $M = 4\pi\rho_s R^3/3$ and g is the gravitational acceleration. Considering that the sphere acceleration $\ddot{x}$ is constant and equals the fitted value a, eq. (1) leads to an estimate of the granular friction F_d. Figure 3(b) shows F_d/Mg as a function of α for different sphere diameters and densities. As a general trend, F_d increases both with α and ρ_s and is larger than in the case of pure rolling on a flat and rigid substrate where $F_d = 2/7Mg\sin\alpha$ (black solid line and open dots in fig. 3(b)).

The rolling of the sphere on the granular bed pushes away excess granular material which results in the formation of a characteristic groove as discussed by Crassous *et al.* [9]. In order to characterize the features of the groove, we follow the profile of the granular bed with a laser sheet that intercepts the surface with an oblique incidence, as depicted in fig. 1. A top view of the groove boundary is shown in fig. 4. We first observe that for a given experiment, the depth of the groove δ and its width w, both remain unchanged along the path of the sphere. These results can be attributed to the fact that for $\alpha < 22^\circ$ the sphere displacement does not trigger avalanches but only a local flow of grains. Conversely, for $22^\circ < \alpha < 23^\circ$, the deposition of the sphere induces global avalanches, a regime that lays out of the scope of this study. We then investigate the dependence of δ and w on the radius of the sphere for a given density (fig. 5(a), (b)). One notices that the groove depth and width both increase proportionally to R. Furthermore, the detailed study of the geometry of the groove as a function of the slope α for a given sphere (fig. 6(a), (b)) shows that both δ and w remain nearly independent of α, for the range of angles accessible in the experiments ($\alpha < 22^\circ$).

Model. – We first focus on the features of a groove produced by a sphere that is gently deposited on a flat and horizontal granular surface. Uehara *et al.* investigated

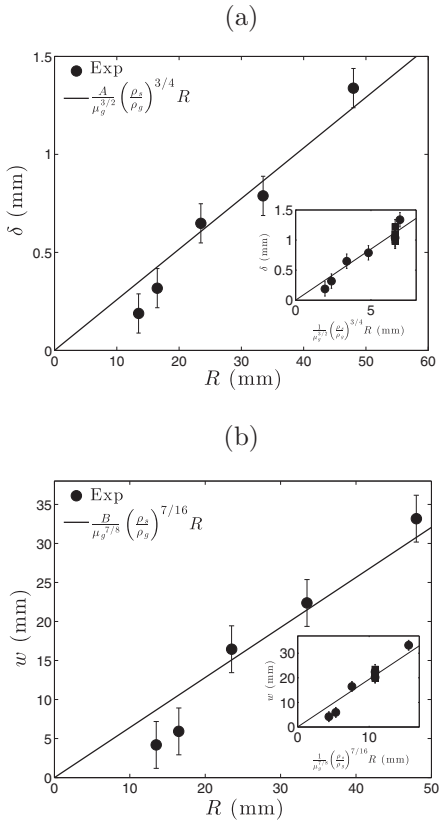

Fig. 5: Depth (a) and width (b) of the groove formed by the passage of a sphere as a function of the radius of the sphere for a given density $\rho_s = 22\,\mathrm{kg/m^3}$. Dots correspond to experimental data and black solid lines to the predictions of eqs. (2) and (3) for $\rho_s/\rho_g = 22/1540$, $\mu_g = 0.40$, $A = 0.16$ and $B = 1.94$. The insets show the data for two ball densities, $\rho_s = 22\,\mathrm{kg/m^3}$ (dots) and $\rho_s = 57\,\mathrm{kg/m^3}$ (squares). (a) δ as a function of $(\rho_s/\rho_g)^{3/4}R/\mu_g^{3/2}$. (b) w as a function of $(\rho_s/\rho_g)^{7/16}R/\mu_g^{7/8}$.

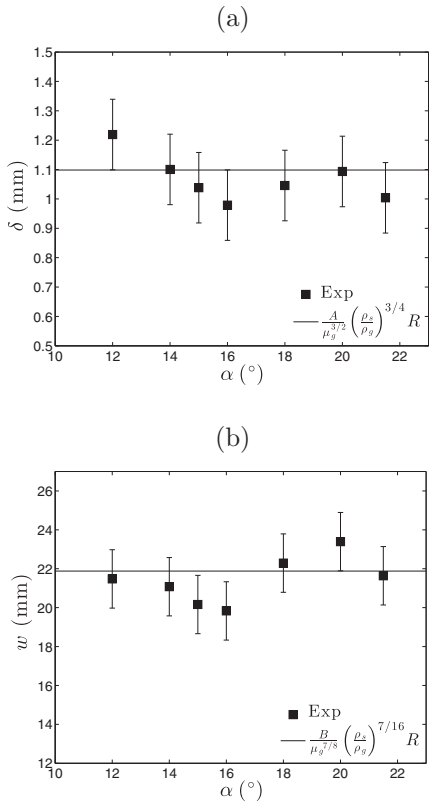

Fig. 6: Depth (a) and width (b) of the groove left after the passage of a sphere as a function of the slope angle α for a sphere of radius $R = 22\,\mathrm{mm}$ and density $\rho_s = 57\,\mathrm{kg/m^3}$. Squares correspond to experimental data and black solid lines to the predictions of eqs. (2) and (3) for $\rho_s/\rho_g = 57/1540$, $\mu_g = 0.40$, $A = 0.16$ and $B = 1.94$.

the depth and the diameter of a crater formed by a sphere impacting a granular medium at low speed [12]. In the limit of sphere released just above the medium, the depth and the width of the crater read

$$\delta = \frac{A}{\mu_g^{3/2}}\left(\frac{\rho_s}{\rho_g}\right)^{3/4} R, \tag{2}$$

$$w = \frac{B}{\mu_g^{7/8}}\left(\frac{\rho_s}{\rho_g}\right)^{7/16} R, \tag{3}$$

where μ_g is the friction coefficient between grains (for the glass beads used in our experiments, $\mu_g = 0.40$, as deduced from the angle of repose of a granular pile) and A, B are numerical coefficients. Adjusting eqs. (2) and (3) to the experimental data, we find that the best fits are obtained for $A = 0.16$ and $B = 1.94$ (solid lines in figs. 5 and 6). These values hold for the two sphere densities considered in this study (insets in figs. 5(a) and (b)). The numerical values of A and B differ from the ones measured by Uehara *et al.* for the case of crater impacts ($A = 0.13$ and $B = 0.93$) [12]. We attribute this difference to the fact that the contact area between the rolling sphere and the grains is lower than the area of a sphere at rest.

Hereafter, we develop an empirical model for the granular friction experienced by the sphere. While rolling downwards, the sphere is in contact with grains on a zone characterized by the angle θ_m given by $\cos\theta_m = 1 - \delta/R$ (fig. 7). In a continuum approach, normal and tangential stresses are distributed along the contact zone. These stress distributions can be reduced to two punctual forces along the radial and orthoradial direction, denoted f_r and f_θ, respectively. The orientation of f_r and f_θ relatively to the slope defines the angle θ_c (fig. 7). The static equilibrium of the sphere thus corresponds to $\theta_c = \alpha$, $f_r = -Mg$ and $f_\theta = 0$. For the case of rolling motion, we propose a heuristic expression of θ_c as a function of θ_m and α, $\theta_c = \theta_m(1 - e^{-c\alpha/\theta_m})$. This expression includes a progressive loss of symmetry of the stress distribution for increasing α above α_c and the saturation of θ_c to θ_m for large enough α. Indeed, the center of mass of the stress distribution cannot exceed the size of the contact zone. Note that the proposed expression only includes a single adjustable parameter denoted c. Following this expression of θ_c, the critical slope angle α_c for which the sphere starts rolling respects $\alpha_c/\theta_m = 1 - e^{-c\,\alpha_c/\theta_m}$.

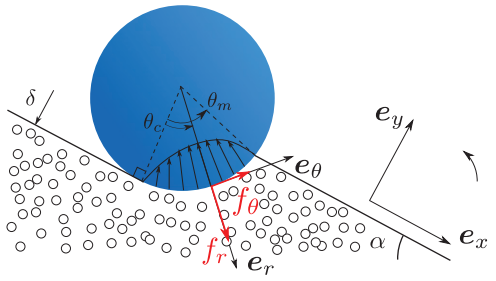

Fig. 7: (Color online) Notations used in the model.

Along the y-direction, f_r and f_θ projections compensate the weight of the sphere, leading to

$$-f_r \cos\theta_c + f_\theta \sin\theta_c = Mg\cos\alpha. \tag{4}$$

Along the x-direction, the projections of f_r and f_θ define the friction force F_d experienced by the sphere,

$$F_d = -f_r \sin\theta_c - f_\theta \cos\theta_c. \tag{5}$$

Finally, the torque equilibrium toward the center of the sphere yields

$$J\ddot{\theta} = Rf_\theta, \tag{6}$$

where $J = 2/5MR^2$ is the moment of inertia of a homogeneous sphere relatively to the sphere centered axis. Measurements of the sphere rotation indicate that the non-sliding approximation holds in our experiments (fig. 3(a)). Thus, the non-sliding relation, $R\dot{\theta} = -\dot{x}$, combined with eqs. (1) and (6) leads to

$$f_\theta = -\frac{J}{MR^2}(Mg\sin\alpha - F_d), \tag{7}$$

which along with eqs. (4), (5) yields to the reduced friction force

$$\frac{F_d}{Mg} = \cos\alpha\left(\frac{\frac{2}{5}\tan\alpha + \sin\theta_c}{\frac{2}{5} + \cos\theta_c}\right), \tag{8}$$

where $\theta_c = \theta_m(1 - e^{-c\alpha/\theta_m})$, $\cos\theta_m = 1 - \delta/R$, and δ is given by eq. (2). Equation (8) predicts that F_d/Mg increases with the slope angle α and the density ratio ρ_s/ρ_g and does not depend on the sphere radius R. These trends are in qualitative agreement with the observations previously made (fig. 3(b)). Thereafter, the experimental data have been adjusted to the theoretical predictions of the normalized friction force F_d/Mg deduced from eq. (8). The best fit of the data is provided for $c = 1.5$ as represented by blue and yellow solid lines in fig. 3(b). The good agreement with experiments justifies *a posteriori* the assumption made on the dependence of θ_c with θ_m and α. Indeed, the experimental data could not be captured by an empirical law where θ_c depends solely on θ_m. Moreover, the fact that a same value of the coefficient c allows to fit different density ratios ρ_s/ρ_g suggests that c does not depend on the properties of the granular bed. In addition, we performed similar experiments on a sand bed ($\rho_g = 1549\,\mathrm{kg/m^3}$ and $\mu_g = 0.65$) and a good agreement between the theory and the experiments has been obtained when the physical properties of the sand are considered. Finally, the fit of the predictions with experimental data provides a first characterization of the distribution of contact forces and its dependence with the properties of the granular medium and the slope angle.

Discussion. – Following eq. (8), we deduce that the dynamics of the rolling sphere on a deformable granular slope is equivalent to the dynamics of a sphere rolling over a non-deformable incline with a friction coefficient $\mu_{\mathrm{eff}} = (\frac{2}{5}\tan\alpha + \sin\theta_c)/(\frac{2}{5} + \cos\theta_c)$. This observation justifies the De Blasio and Saeter assumption of interpreting the deceleration of a sphere on a granular slope in terms of effective friction coefficients [10]. In their experiments, an increase of the effective friction coefficient with the slope angle was observed, a fact which is in agreement with the predictions of eq. (8). However, a direct comparison with our model is not possible because the internal friction coefficient of their grains was not provided. Note that the expression of μ_{eff} depends on the properties of the granular medium through its bulk density and its internal friction coefficient. The larger the values of ρ_g and μ_g, the lower the normalized granular friction F_d/Mg. We thus expect the compaction of the granular medium to reduce the friction of the rolling sphere. This fact was verified experimentally by tapping several times the granular preparation prior to the release of the sphere.

Thereafter, we apply our results to estimate the force required for beetles to push dung balls over sandy surfaces. Considering $\rho_g \sim 1500\,\mathrm{kg/m^3}$, $\mu_g \sim 0.7$ and assuming that the dung ball density is $\rho_b \sim 800\,\mathrm{kg/m^3}$, the force required to roll the dung ball on a flat and sandy ground is equal to about a fifth of the ball weight. For a dung ball that is 50 times the weight of the insect as measured by Bartholomew and Heinrich [3], a beetle must be able to generate forces about 10 times its own weight in order to move the dung ball. The maximal pushing force of beetles belonging to the *Scarabaeidae* family, has been reported by Evans and Forsythe to be about 250 times their own weight [13], thus ball rolling is not the hardest tasks that dung beetles can complete.

In this work, we only considered the case of high contrast in density where the rolling sphere induces a surrounding granular flow. However, our predictions do not hold for low density ratio where the penetration depth δ becomes lower than the grain size ($\delta < d$), a fact that occurs for $\rho_s/\rho_g < 11\mu_g^2(d/R)^{4/3}$ according to eq. (2). In this limit, the granular bed acts as a non-deformable rough substrate for the rolling sphere. Such a situation has been investigated by Tardivel *et al.* with balls decelerating on a flat granular bed [2]. In their experiments, they used a basket ball of radius $R = 119\,\mathrm{mm}$ and density $\rho_s = 89\,\mathrm{kg/m^3}$ and a medicine ball of radius $R = 113\,\mathrm{mm}$ and density $\rho_s = 447\,\mathrm{kg/m^3}$. The granular bed is made of grains of size ranging from 6 to 12 mm with an internal

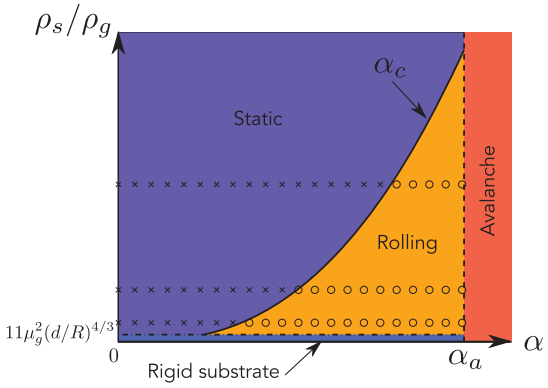

Fig. 8: (Color online) Diagram of the different regimes encountered by a sphere placed on a granular bed made of glass beads as a function of its angle α and the density ratio between the sphere and the grains ρ_s/ρ_g. Crosses and dots indicate, respectively, the non-rolling and rolling situations observed experimentally for spheres of respective density $\rho_s = 21$, 57 and 171 kg/m^3.

friction coefficient $\mu_g = 0.87$. In such conditions, the penetration depth δ predicted by eq. (2) is less than 2 mm, thus lower than a third of the minimal grain size. In order to approach this limit, Tardivel *et al.* developed a model based on a succession of micro-collisions on a rigid surface with small asperities. Such a model yields an expression for the effective friction coefficient $\mu_{\text{eff}} = MR^2/J\sqrt{d/2R}$ which predicts the experimental value within a precision of 25%.

Finally, the different behaviors of a sphere placed on a granular slope are summarized in fig. 8. Stable granular slopes are encountered for angles smaller than the avalanche angle α_a (below the vertical dashed line). For small density ratio $\rho_s/\rho_g < 11\mu_g^2(d/R)^{4/3}$, the granular bed remains undeformed and behaves like a rough surface as described by Tardivel *et al.* [2] (below the horizontal dotted line). At small slope angles $\alpha < \alpha_c$ or large density ratio, the sphere is in static equilibrium in the crater formed by its release (above the solid line which represents the solution of the relation $\alpha_c/\theta_m = 1 - e^{-c\alpha_c/\theta_m}$ that leads to $\alpha_c \simeq 0.61\theta_m$ for $c = 1.5$). Between these three limits, the sphere rolls down while deforming the granular bed as considered in the present study.

Conclusion. – This study investigated the dynamics of a sphere rolling down a granular slope. While moving down, the sphere displaces grains and leaves a track, inducing a granular friction. Remarkably, the sphere follows a uniformly accelerated motion within the range of experimental parameters explored in this work. We estimated the steady friction force from the dynamics of the sphere and showed that it increases with the sphere density and the slope angle. The depth and the width of the groove created by the sphere were characterized experimentally and approached by the laws established in the case of a sphere impacting a granular bed at zero falling height. Thereafter, a mechanical model of the rolling sphere on a granular slope has been developed. Although this model is based on a heuristic description of the distribution of the contact forces between the rolling sphere and the granular bed, the comparison with experiments is fairly good. Finally, this model provides crucial information on the distribution of contact forces and its dependence on the slope angle.

* * *

The authors thank Fivos Pham for preliminary experiments. FM acknowledges support from Proyecto Fortalecimiento USACH USA1799-MF072215.

REFERENCES

[1] De Blasio F. V. and Sæter M.-B., *Earth Surf. Process. Landforms*, **40** (2015) 599.
[2] Van wal S., Tardivel S., Sánchez P., Djafari-Rouhani D. and Scheeres D., *Granular Matter*, **19** (2017) 17.
[3] Bartholomew G. A. and Heinrich B., *J. Exp. Biol.*, **73** (1978) 65.
[4] Antol J., Calhoun P., Flick J., Hajos G., Kolacinski R., Minton D., Owens R. and Parker J., *Low cost Mars surface exploration: The Mars tumbleweed*, NASA Technical Report (2003).
[5] Wilson J. L., Mazzoleni A. P., DeJarnette F. R., Antol J., Hajos G. A. and Strickland C. V., *J. Spacecraft Rockets*, **45** (2008) 370.
[6] Behar A., Matthews J., Carsey F. and Jones J., *Nasa/jpl tumbleweed polar rover*, in *Proceedings of the IEEE Aerospace Conference, 2004*, Vol. **1** (IEEE) 2004.
[7] Bekker M. G., Theory of Land Locomotion (University of Michigan Press) 1956.
[8] Bekker M. G., *Off-the-road Locomotion. Research and Development in Terramechanics* (University of Michigan Press) 1960.
[9] Crassous J., Humeau A., Boury S. and Casas J., *Phys. Rev. Lett.*, **119** (2017) 058003.
[10] De Blasio F. V. and Saeter M.-B., *Phys. Rev. E*, **79** (2009) 022301.
[11] Pouliquen O. and Forterre Y., *J. Fluid Mech.*, **453** (2002) 133.
[12] Uehara J. S., Ambroso M. A., Ojha R. P. and Durian D. J., *Phys. Rev. Lett.*, **90** (2003) 194301.
[13] Evans M. E. G. and Forsythe T. G., *J. Zool.*, **202** (1984) 513.